

Wave propagation modeling in cylindrical human long wet bones with cavity

A.M. Abd-Alla · S.M. Abo-Dahab · S.R. Mahmoud

Received: 5 April 2010 / Accepted: 30 November 2010 / Published online: 12 January 2011
© Springer Science+Business Media B.V. 2011

Abstract The wave propagation modeling in cylindrical human long wet bones with cavity is studied. The dynamic behavior of a wet long bone that has been modeled as a piezoelectric hollow cylinder of crystal class 6 is investigated. An analytical solutions for the mechanical wave propagation during a long wet bones have been obtained for the flexural vibrations. The average stresses of solid part and fluid part have been obtained. The frequency equations for poroelastic bones are obtained when the medium is subjected to certain boundary conditions. The dimensionless frequencies are calculated for poroelastic wet bones for various values for non-dimensional wave lengths. The

dispersion curves of the dry bone and wet bone for the flexural mode $n = 2$ are plotted. The numerical results obtained have been illustrated graphically.

Keywords Elastic · Bones · Poroelastic · Transversely isotropic · Mechanical wave · Natural frequency · Piezoelectric material

1 Introduction

The investigation of remodeling properties and smart behavior of bone tissue and their applications to biomedical engineering by considering its coupled elastic, magnetic, electric behavior has received a considerable interest among the scientists of different fields in the past decades. Bone is an heterogeneous and anisotropic natural composite. It is assumed that the solid part is perfectly elastic and the fluid part is Newtonian viscous and compressible. The pores are interconnected and that flow of fluid, produced by deformation of bone is governed by Darcy's law. The study of wave propagation through a continuous media is of practical importance in the field of engineering, medicine and in bioengineering. Application of the poroelastic materials in medicinal fields such as orthopedics, dental and cardiovascular is well known. In macroscopic terms the percentage of porosity in the cortical bone is 3–5%, whereas in the trabecular or cancellous the percentage of porosity is up to 90%

A.M. Abd-Alla · S.M. Abo-Dahab (✉)
Maths. Dept., Faculty of Science, Taif University, Taif,
Saudi Arabia
e-mail: sdahb@yahoo.com

A.M. Abd-Alla
e-mail: mohmrr@yahoo.com

A.M. Abd-Alla · S.R. Mahmoud
Maths. Dept., Faculty of Science, Sohag University, Sohag,
Egypt

S.R. Mahmoud
e-mail: samsam73@yahoo.com

S.R. Mahmoud
Maths. Dept., Faculty of Education, King Abdul Aziz
University, Jeddah, Saudi Arabia

S.M. Abo-Dahab
Maths. Dept., Faculty of Science, SVU, Qena 83523, Egypt

(see, Natali and Meroi [1]). In recent years, noninvasive quantitative ultrasound (QUS) techniques have become important modalities for the investigation of bone strength by Natali and Meroi [1], Thompson et al. [2], Doherty et al. [3], Jurist [4] and Papatthanasopoulou et al. [5]. The measurement of ultrasonic properties of bone such as the speed of sound (SOS) or the slope of frequency-dependent attenuation (broadband ultrasonic attenuation BUA) using the transmission of elastic wave through the skeleton has been shown to convey important information related to bone strength.

The dynamical behavior model, especially, wave propagation and vibration of bone are necessary in measuring *in vivo* properties of bone by the above noninvasive method which discussed by Thompson et al. [2], Doherty et al. [3] and Jurist [4], Papatthanasopoulou et al. [5] investigated a theoretical analysis of the internal bone remodeling process induced by a medullar pin is presented. Fotiadis et al. [6] studied wave propagation in human long wet bones of arbitrary cross-section. Fotiadis et al. [7] presented wave propagation modeling in human long wet bones. Sebaa et al. [8] considered many applications of fractional calculus to ultrasonic wave propagation in human cancellous bone. Padilla et al. [9], studied numerically the problem of wave propagation in cancellous bone. Haeat et al. [10] investigated numerical simulation of the dependence of quantitative ultrasonic parameters on trabecular bone's micro-architecture and elastic constants. Pithious et al. [11] presented, an alternative ultrasonic method for measuring the elastic properties of cortical bone. Kaczmarek et al. [12] investigated short ultrasonic waves in cancellous bone. Levitsky et al. [13] studied wave propagation in cylindrical viscous layer between two elastic shells. Tadeu et al. [14] studied 3D elastic wave propagation modelling in the presence of 2D fluid-filled thin inclusions. Paul and Murali [15] investigated wave propagation in a cylindrical poroelastic bone with cavity. wet bones are heterogeneous and an isotropic in nature. Qin et al. [16] studied thermoelectroelastic solutions for surface bone remodeling under axial and transverse loads.

Protopappas et al. [25] studied the ultrasonic monitoring of bone fracture healing, quantitative ultrasound has attracted significant interest in the evaluation of bone fracture healing, animal and clinical studies have demonstrated that the propagation velocity across fractured bones can be used as an indicator of healing.

Ultrasound velocity measurements on healing bones using the external fixation pins: a two-dimensional simulation study is pointed out by Vavva et al. [26]. The problem of computer simulations in the ultrasonic characterization of bone has further extended our understanding about the parameters that affect ultrasound velocity measurements is investigated by Kauffman [27] and Moilanen [28]. Vavva et al. [29] illustrated the velocity dispersion of guided waves propagating in a free gradient elastic plate: Application to cortical bone. Recently, Mahmoud [24] pointed out the wave propagation in cylindrical poroelastic dry bones.

In the present paper, the three-dimensional equations of elastodynamics for transversely isotropic media are solved in terms of three displacement potentials, each satisfying a partial differential equation of the second order. For the hollow circular cylinder, subjected to certain boundary conditions (fixed and mixed boundary conditions), the results obtained in a characteristic frequency equation in determinantal form of sixth order. Several special cases of the general frequency equation are discussed, including axially symmetric wave motion, the limiting modes of infinite wave length, and longitudinal waves in a long thin solid cylinder. The analysis presented here parallels the work of Fotiadis et al. [7] who studied the corresponding problem for hollow transversely isotropic circular cylinders. The paper is classified as follows. In Sect. 2, we present the formulation of the problem. The solution of mechanical equation as harmonic wave in hollow cylinder of infinite extent is derived in Sect. 3. In Sect. 4, we investigate the frequency equation taking into consideration the boundary conditions, inner surface fixed and outer surface fixed. Some special cases are discussed in Sect. 5. The frequency equation in solid circular cylinder is investigated in Sect. 6. The numerical results of the frequency equation are discussed in detail for wet bones, displayed graphically and discussed in Sect. 7. Finally, the conclusions are introduced in Sect. 8.

2 Formulation of the mechanical waves

The constitutive equations for a transversely isotropic case with z as axis of the symmetry are taken in polar coordinates as in Biot [17] take the form

$$\left. \begin{aligned}
 \sigma_{rr} &= C_{11} \frac{\partial u_r}{\partial r} + C_{12} \frac{1}{r} \left(u_r + \frac{\partial u_\theta}{\partial \theta} \right) + C_{13} \frac{\partial u_z}{\partial z} + M \left[\frac{\partial v_r}{\partial r} + \frac{1}{r} \frac{\partial v_\theta}{\partial \theta} + \frac{\partial v_z}{\partial z} \right], \\
 \sigma_{\theta\theta} &= C_{12} \frac{\partial u_r}{\partial r} + C_{11} \frac{1}{r} \left(u_r + \frac{\partial u_\theta}{\partial \theta} \right) + C_{13} \frac{\partial u_z}{\partial z} + M \left[\frac{\partial v_r}{\partial r} + \frac{1}{r} \frac{\partial v_\theta}{\partial \theta} + \frac{\partial v_z}{\partial z} \right], \\
 \sigma_{zz} &= C_{13} \left[\frac{\partial u_r}{\partial r} + \frac{1}{r} \left(u_r + \frac{\partial u_\theta}{\partial \theta} \right) \right] + C_{33} \frac{\partial u_z}{\partial z} \\
 &\quad + Q \left[\frac{\partial v_r}{\partial r} + \frac{1}{r} \left(v_r + \frac{\partial v_\theta}{\partial \theta} \right) + \frac{\partial v_z}{\partial z} \right], \\
 \sigma_{\theta z} &= C_{44} \left[\frac{\partial u_\theta}{\partial z} + \frac{1}{r} \frac{\partial u_z}{\partial \theta} \right], \quad \sigma_{rz} = C_{44} \left[\frac{\partial u_r}{\partial z} + \frac{\partial u_z}{\partial r} \right], \\
 \sigma_{r\theta} &= C_{66} \left[\frac{\partial u_\theta}{\partial r} + \frac{1}{r} \left(\frac{\partial u_r}{\partial \theta} - u_\theta \right) \right], \\
 \sigma &= M \left[\frac{\partial u_r}{\partial r} + \frac{1}{r} \left(\frac{\partial u_\theta}{\partial \theta} + u_r \right) \right] + Q \frac{\partial v_z}{\partial z} + R \left[\frac{\partial v_r}{\partial r} + \frac{1}{r} \left(v_r + \frac{\partial v_\theta}{\partial \theta} \right) + \frac{\partial v_z}{\partial z} \right]
 \end{aligned} \right\} \tag{2.1}$$

where, σ_{ij} and σ are the average stresses of solid and fluid respectively and C_{ij} , M , Q , R are the elastic constants and $C_{66} = \frac{1}{2}(C_{11} - C_{12})$.

The equation of the flow is

$$b_{rr}^{-1} \nabla^2 \sigma + b_{zz}^{-1} \sigma = \frac{\partial(\varepsilon - \sigma)}{\partial t} \tag{2.2}$$

where, $b_{rr} = \frac{\mu f^2}{k_{rr}}$, $b_{zz} = \frac{\mu f^2}{k_{zz}}$, ∇^2 is Laplacian operator in polar coordinates, μ is the viscosity, f is the porosity and k_{rr} , k_{zz} are the permeability of the medium. The average displacements of solid and velocity of fluid phases are taken as u_i , and v_i respectively. The strains are expressed as $e_{ij} = \frac{1}{2}(u_{i,j} + u_{j,i})$ and dilation of the phases as $e = u_{i,j}$ and $\varepsilon = v_{i,i}$.

In general the stress-strain relation for a piezoelectric body can be written in the following way in matrix notation

$$\sigma_m = C_{mn} S_n - e_{mk} E_k, \quad 1 \leq m, n \leq 6, \quad 1 \leq k \leq 3 \tag{2.3}$$

where, e_{mk} and E_k are, respectively, the piezoelectric strain constants and the components of the electrical field. The last term in (2.3) is ignored in (2.1) for simplification purposes the calculation. But this step can

be justified, where, they showed that the piezoelectric stiffening in bones in the ultrasonic wave propagation is small and negligibly. This simplification leads to the mechanical stress equations by using the three dimensional stress equations of motion in the form

$$\left. \begin{aligned}
 \frac{\partial \sigma_{rr}}{\partial r} + \frac{1}{r} \frac{\partial \sigma_{r\theta}}{\partial \theta} + \frac{\partial \sigma_{rz}}{\partial z} + \frac{1}{r} (\sigma_{rr} - \sigma_{\theta\theta}) &= \rho \frac{\partial^2 u_r}{\partial t^2}, \\
 \frac{\partial \sigma_{r\theta}}{\partial r} + \frac{1}{r} \frac{\partial \sigma_{\theta\theta}}{\partial \theta} + \frac{\partial \sigma_{\theta z}}{\partial z} + \frac{2}{r} \sigma_{\theta r} &= \rho \frac{\partial^2 u_\theta}{\partial t^2}, \\
 \frac{\partial \sigma_{rz}}{\partial r} + \frac{1}{r} \frac{\partial \sigma_{\theta z}}{\partial \theta} + \frac{\partial \sigma_{zz}}{\partial z} + \frac{1}{r} \sigma_{zr} &= \rho \frac{\partial^2 u_z}{\partial t^2}
 \end{aligned} \right\} \tag{2.4}$$

where, ρ is the density of the bone and t is the time.

3 Solution of the mechanical equations

In this analysis, a long bone is approximated by an infinite hollow cylinder. The free harmonic wave in hollow cylinder of infinite extent can be obtained by using

the following solution in the field equations:

$$\left. \begin{aligned} u_r(r, \theta, z, t) &= \left[\frac{\partial \Phi}{\partial r} + \frac{1}{r} \frac{\partial \Psi}{\partial \theta} \right] e^{i(kz - \varpi t)}, \\ v_r(r, \theta, z, t) &= -\frac{\partial \eta}{\partial r} e^{i(kz - \varpi t)}, \\ u_\theta(r, \theta, z, t) &= \left[\frac{1}{r} \frac{\partial \Phi}{\partial \theta} - \frac{\partial \Psi}{\partial r} \right] e^{i(kz - \varpi t)}, \\ v_\theta(r, \theta, z, t) &= -r^{-1} \frac{\partial \eta}{\partial \theta} e^{i(kz - \varpi t)}, \\ u_z(r, \theta, z, t) &= \left[\frac{iw}{h} \right] e^{i(kz - \varpi t)}, \\ v_z(r, \theta, z, t) &= -ik\eta e^{i(kz - \varpi t)} \end{aligned} \right\} \quad (3.1)$$

where, $u_r, u_\theta, u_z, v_r, v_\theta,$ and v_z are mechanical displacements and velocities, $k, \varpi,$ and h are the wave number, frequency and thickness of the cylinder, $h = b - a,$ a is the inner radius, b is the outer radius and Φ, Ψ, ζ and η all values are functions of r and θ only.

Substituting from (2.1) into (2.2), (2.4) and using (3.1), we obtain:

$$\left. \begin{aligned} (C_{11}\nabla^2 + \rho\varpi^2 - k^2C_{44})\Phi - (C_{44} + C_{13})\left(\frac{k\zeta}{h}\right) \\ - M(\nabla^2 - k^2)\eta = 0, \\ (C_{44}\nabla^2 + \rho\varpi^2 - k^2C_{33})\left(\frac{\zeta}{h}\right) \\ + (C_{44} + C_{13})k\nabla^2\Phi + kQ(\nabla^2 - k^2)\eta = 0, \\ \left\{ M\left[\frac{\nabla^4}{b_{rr}} - \frac{k^2\nabla^2}{b_{zz}}\right] + i\varpi\nabla^2 \right\} \Phi \\ + \left\{ \left(\frac{Q}{h}\right)\left[\frac{-k\nabla^2}{b_{rr}} + \frac{k^3}{b_{zz}}\right] - \frac{i\varpi k}{h} \right\} \zeta \\ + \left\{ R\left[\frac{-\nabla^2(\nabla^2 - k^2)}{b_{rr}} + \frac{k^2(\nabla^2 - k^2)}{b_{zz}}\right] \right. \\ \left. + i\varpi(\nabla^2 - k^2) \right\} \eta = 0, \\ (C_{66}\nabla^2 + \rho\varpi^2 - k^2C_{44})\Psi = 0. \end{aligned} \right\} \quad (3.2)$$

By defining the dimensionless coordinate $x = \frac{r}{h}$ and $\varepsilon_1 = kh,$ the above equations are written in dimension-

less parameter x and ε_1 as:

$$\left. \begin{aligned} (\bar{C}_{11}\nabla^2 + (ch)^2 - \varepsilon_1^2)\Phi - (1 + \bar{C}_{13})(\varepsilon_1\zeta) \\ - \bar{M}\xi = 0, \\ (1 + \bar{C}_{13})\varepsilon_1\nabla^2\Phi + (\nabla^2 + (ch)^2 - \varepsilon_1^2\bar{C}_{33})\zeta \\ - \varepsilon_1Q\xi = 0, \\ \nabla^2(\nabla^2 - b\varepsilon_1^2 + iD)\Phi \\ - \varepsilon_1(Q'\nabla^2 + bQ'\varepsilon_1^2 - iD)\zeta \\ + (-R'\nabla^2 + bR'\varepsilon_1^2 + iD)\xi = 0, \end{aligned} \right\} \quad (3.3)$$

$$(\bar{C}_{66}\nabla^2 + (ch)^2 - \varepsilon_1^2)\Psi = 0 \quad (3.4)$$

where,

$$\begin{aligned} \xi &= (\nabla^2 - k^2)\eta, & D &= \frac{\varpi h^2 b_{rr}}{M}, & Q' &= \frac{Q}{M}, \\ R' &= \frac{R}{M}, & \bar{M} &= \frac{M}{C_{44}}, & \bar{Q} &= \frac{Q}{C_{44}}, \\ c^2 &= \frac{\rho\varpi^2}{C_{44}}, & b &= \frac{b_{rr}}{b_{zz}}, & \bar{C}_{ij} &= \frac{C_{ij}}{C_{44}}, \\ \nabla^2 &= \frac{\partial^2}{\partial x^2} + \frac{1}{x} \frac{\partial}{\partial x} + \frac{1}{x^2} \frac{\partial^2}{\partial \theta^2}, & (i, j &= 1, 2, 3). \end{aligned}$$

The reason for ξ being defined as above and not being solved for the variable η is that the flow of fluid through the boundaries of bone does not take place during the study of the propagation of waves. However, η can be calculated if the flow on the boundaries is prescribed writing (3.3) in the form

$$\begin{pmatrix} (\bar{C}_{11}\nabla^2 + \bar{A}) & -\bar{B} & -\bar{M} \\ \bar{B}\nabla^2 & (\nabla^2 + \bar{C}) & -\bar{Q}\varepsilon_1 \\ T_1 & T_2 & T_3 \end{pmatrix} \begin{pmatrix} \Phi \\ \zeta \\ \xi \end{pmatrix} = (0)$$

where,

$$\begin{aligned} T_1 &= \nabla^2(\nabla^2 - b\varepsilon_1^2 + iD), \\ T_2 &= -\varepsilon_1(Q'\nabla^2 + bQ'\varepsilon_1^2 - iD), \\ T_3 &= (-R'\nabla^2 + \bar{b}R'\varepsilon_1^2 + iD), & A &= (ch)^2 - \varepsilon_1^2, \\ \bar{B} &= (1 + \bar{C}_{13})\varepsilon_1, & \bar{C} &= (ch)^2 - \varepsilon_1^2\bar{C}_{33}. \end{aligned}$$

Evaluating the determinantal form, the following equations are obtained

$$(\nabla^6 + P\nabla^4 + G\nabla^2 + H)(\Phi, \zeta, \xi) = 0 \quad (3.5)$$

$$\begin{aligned}
 P &= \frac{R'\varepsilon_1^2\bar{C}_{11} + iD\bar{C}_{11} + \bar{C}R'\bar{C}_{11} - \bar{Q}\bar{Q}\varepsilon_1^2\bar{C}_{11} + \bar{A}R' - \bar{B}^2R' + BQ'\varepsilon_1 + \bar{M}\varepsilon_1^2}{-R'\bar{C}_{11} + \bar{M}} \\
 &\quad + \frac{-\bar{Q}\varepsilon_1B + i\bar{M}D + \bar{M}D}{-R'\bar{C}_{11} + \bar{M}}, \\
 G &= \frac{CR'\varepsilon_1^2\bar{C}_{11} + iDC\bar{C}_{11} + Q'\varepsilon_1^4\bar{Q}\bar{C}_{11} - iD\bar{Q}\varepsilon_1^2\bar{C}_{11} + \bar{A}R'\varepsilon_1^2 + i\bar{A}D + \bar{A}CR'}{-R'\bar{C}_{11} + \bar{M}} \\
 &\quad + \frac{-\bar{A}Q'\bar{Q}\varepsilon_1^2 + BD\varepsilon_1^3 - iD\varepsilon_1 + C\varepsilon_1^2 - \bar{B}\bar{Q}\varepsilon_1^3 + iDB\varepsilon_1\bar{M} + iDC\bar{M} - \bar{M}C\varepsilon_1^2}{-R'\bar{C}_{11} + \bar{M}}, \\
 H &= \frac{CR'\varepsilon_1^2 + iDC + \bar{Q}\varepsilon_1^4Q' - iD\bar{Q}\varepsilon_1^2}{-R'\bar{C}_{11} + \bar{M}}A.
 \end{aligned}$$

The solutions of (3.5) can be written as:

$$\left. \begin{aligned}
 \Phi &= \sum_{i=1}^3 [A_i J_n(\alpha_i x) + B_i Y_n(\alpha_i x)] \cos n\theta, \\
 \zeta &= \sum_{i=1}^3 d_i [A_i J_n(\alpha_i x) + B_i Y_n(\alpha_i x)] \cos n\theta, \\
 \xi &= \sum_{i=1}^3 e_i [A_i J_n(\alpha_i x) + B_i Y_n(\alpha_i x)] \cos n\theta
 \end{aligned} \right\} \quad (3.6)$$

where, α_i^2 are the non-zero roots of the equation: $\alpha^6 - P\alpha^4 + G\alpha^2 - H = 0$ and d_i and e_i are given by,

$$\begin{aligned}
 &\left((1 + \bar{C}_{13})\varepsilon_1 d_i + \bar{M}e_i = \bar{C}_{11}\alpha_i^2 - (ch)^2 - \varepsilon_1^2 \right), \\
 &\left(-\alpha_i^2 + (ch)^2 - \varepsilon_1^2 \bar{C}_{33} \right) d_i - \bar{Q}\varepsilon_1 e_i = (1 + \bar{C}_{13})\varepsilon_1 \alpha_i^2
 \end{aligned}$$

the solution of (3.4) takes the form

$$\Psi = [A_4 J_n(\alpha_4 x) + B_4 Y_n(\alpha_4 x)] \sin n\theta \quad (3.7)$$

where, $\alpha_4^2 = \frac{((ch)^2 - \varepsilon_1^2)}{C_{66}}$.

4 Frequency equation

4.1 Fixed boundary conditions

Using the following boundary conditions, inner surface fixed and outer surface fixed

$$\left. \begin{aligned}
 u_r = u_\theta = u_z = \sigma = 0 &\quad \text{at } r = a, \\
 u_r = u_\theta = u_z = \sigma = 0 &\quad \text{at } r = b.
 \end{aligned} \right\} \quad (4.1)$$

Substituting from (3.1), (3.6) and (3.7) into (4.1) and grouping the coefficients of A_1, B_1, A_2, B_2, A_3 and B_3 , we get the characteristic frequency equation as a determinant form as

$$|a_{ij}| = 0, \quad (i, j = 1, 2, \dots, 8) \quad (4.2)$$

where, the coefficients of a_{ij} are included in Appendix A in the paper end.

In this study, the wave propagation of a wet bone with circular cylindrical cavity subjected to inner fixed surface ($r = a$) and outer fixed surface ($r = b$) is considered, the frequency equation is obtained by considering the material as transversely isotropic in nature.

The numerical results are carried out and compared for the wet bone as a poroelastic material and a purely transversely isotropic elastic material.

For very large wave numbers, dispersion curves for flexural modes ($n = 1, 2$) deviate. The derivation of η from ζ will lead to two arbitrary constants which can be calculated if the pores of the bone at $r = a, b$ are shielded, that is

$$\frac{\partial \eta}{\partial r} = 0 \quad \text{at } r = a, b.$$

4.2 Mixed boundary conditions

Using the following, boundary conditions, outer surface free and inner surface fixed.

$$\left. \begin{aligned}
 \sigma_{rr} = \sigma_{rz} = \sigma_{r\theta} = \sigma = 0 &\quad \text{at } r = b, \\
 u_r = u_\theta = u_z = \sigma = 0 &\quad \text{at } r = a
 \end{aligned} \right\} \quad (4.3)$$

where, $\bar{a} = a/h, \bar{b} = b/h$.

Substituting from (3.1), (3.6) and (3.7) into (4.3) and grouping the coefficients of A_1, B_1, A_2, B_2, A_3 ,

B_3 , A_4 and B_4 , we obtain the characteristic frequency equation as the determinant form

$$|a_{ij}| = 0 \quad (i, j = 1, 2, 3, \dots, 8) \tag{4.4}$$

where, the coefficients of a_{ij} are take the form in Appendix B in the paper end.

In this study, the wave propagation of a wet bone with circular cylindrical cavity subjected to traction free inner surface ($r = b$) and fixed surface ($r = a$) is considered, the frequency equation is obtained by considering the material as transversely isotropic in nature.

The numerical results are carried out and compared for the wet bone as a poroelastic material and a purely transversely isotropic elastic material.

For very large wave lengths, dispersion curves for flexural modes ($n = 1, 2$) deviate.

5 Special cases of frequency equation

5.1 Motion independent of z

As the wave number $k \rightarrow 0$ (i.e., for infinite wave length, $\lambda = 2\pi/k$), the following simplifications result.

$$\left. \begin{aligned} \gamma_1 &\rightarrow \left[\frac{\rho w^2}{C_{11}} \right]^{\frac{1}{2}}, & \gamma_2 &\rightarrow \left[\frac{\rho w^2}{C_{11}} \right]^{\frac{1}{2}}, \\ \lambda_1 k &\rightarrow -k^2(C_{44} + C_{13})/(C_{11} - C_{44}), \\ \lambda_2 k &\rightarrow \rho k^2(C_{44} - C_{13})/C_{44}(C_{11} + C_{44}), \\ k/(\lambda_2 - k) &\rightarrow 0, & (\lambda_1 - k)/(\lambda_2 - k) &\rightarrow 0 \end{aligned} \right\} \tag{5.1}$$

hence,

$$a_{11} = 0 = a_{22} = a_{23} = a_{24} = a_{51} = a_{52} = a_{53} = a_{54}$$

and the characteristic equation (4.2) of fixed boundary conditions and (4.4) of mixed boundary conditions, may be written as the product of two determinants

$$\Delta_1 \Delta_2 = 0$$

$$\Delta_1 = \begin{vmatrix} a_{11} & a_{12} & a_{13} & a_{15} & a_{16} & a_{17} \\ a_{21} & a_{22} & a_{23} & a_{25} & a_{26} & a_{27} \\ a_{41} & a_{42} & a_{43} & a_{45} & a_{46} & a_{47} \\ a_{51} & a_{52} & a_{53} & a_{55} & a_{56} & a_{57} \\ a_{61} & a_{62} & a_{63} & a_{65} & a_{66} & a_{67} \\ a_{81} & a_{82} & a_{83} & a_{85} & a_{86} & a_{87} \end{vmatrix} = 0, \tag{5.2}$$

$$\Delta_2 = \begin{vmatrix} a_{34} & a_{38} \\ a_{74} & a_{78} \end{vmatrix} = 0.$$

The elements a_{ij} in (5.2) are given by (4.2) of fixed boundary conditions and (4.4) of mixed boundary conditions, with $k \rightarrow 0$ (i.e., for infinite wave length, $\lambda = 2\pi/k$) and the appropriate simplifications outlined in (5.1). Furthermore, the Z and W are either J or Y functions, in accordance to Table 1 since $\rho\omega^2 > k^2 C_{33}$, when $k \rightarrow 0$ (i.e., for infinite wave length, $\lambda = 2\pi/k$).

The $\Delta_1 = 0$ corresponds to plane-strain vibrations and is equivalent to that for the isotropic cylinder, with the shear constant C_{44} being replaced by C_{66} —this is to be expected since the z -axis is perpendicular to the plane of isotropy. The Δ_2 represents motion involving the axial displacement u_z only, corresponding to longitudinal-shear vibrations. This equation could have been obtained immediately from the displacement equations of equilibrium (2.2) by setting, $u_r = 0 = u_\theta$, $\frac{\partial}{\partial z} = 0$ with the result.

$$C_{44} \left[\frac{\partial^2 u_z}{\partial r^2} + \frac{1}{r} \frac{\partial u_z}{\partial r} + \frac{1}{r^2} \frac{\partial^2 u_z}{\partial \theta^2} \right] = \rho \frac{\partial^2 u_z}{\partial t^2}$$

subject to the boundary conditions $\frac{\partial u_z}{\partial r} = 0$ on $r = a, b$.

It is noted that the plane-strain and longitudinal shear vibrations are uncoupled when $a = 0$ and become coupled for a nonzero of wave number values (i.e., for infinite wave length, $\lambda = 2\pi/k$).

5.2 Motion independent of θ

For motion independent of θ (i.e., $n = 0$), the characteristic (4.2) and (4.4) may again be represented as the product of two determinants Δ_3, Δ_4 , where

$$\Delta_3 \Delta_4 = 0. \tag{5.3}$$

The elements a_{ij} in (5.3) are given by (4.2) of fixed boundary conditions and (4.4) of mixed boundary conditions, with $n = 0$.

Furthermore, the Z and W are either J or Y functions, in accordance to Table 1 since $\rho\omega^2 > k^2 C_{33}$, when $n = 0$.

$$\Delta_3 = \begin{vmatrix} a_{11} & a_{12} & a_{13} & a_{15} & a_{16} & a_{17} \\ a_{21} & a_{22} & a_{23} & a_{25} & a_{26} & a_{27} \\ a_{31} & a_{32} & a_{33} & a_{35} & a_{36} & a_{37} \\ a_{51} & a_{52} & a_{53} & a_{55} & a_{56} & a_{57} \\ a_{61} & a_{62} & a_{63} & a_{65} & a_{66} & a_{67} \\ a_{71} & a_{72} & a_{73} & a_{75} & a_{76} & a_{77} \end{vmatrix} = 0,$$

$$\Delta_4 = \begin{vmatrix} a_{44} & a_{48} \\ a_{84} & a_{88} \end{vmatrix} = 0.$$

The frequency equation Δ_3 represents the coupled radial and axial motions, which are completely uncoupled from the pure torsional motions given by $\Delta_4 = 0$. These frequency equations have been computed approximately, for orthotropic thick shells, which includes transverse isotropy as a special case. The five elastic constants C_{ij} appear in (5.3), however, this equation reduces to that of the special case of isotropy. For purely torsional modes, the frequency $\Delta_4 = 0$ reduces to

$$J_2(\beta_1 a) Y_2(\beta_1 b) - J_2(\beta_1 b) Y_2(\beta_1 a) = 0$$

for $\rho\omega^2 < k^2 C_{44}$ where $\beta_1 = \left| \frac{\rho\omega^2 - C_{44}k^2}{C_{66}} \right|^{1/2}$.

The corresponding frequency equation for $e < \rho\omega^2 / C_{44}k^2 < 1$ is given by

$$I_2(\beta_1 a) K_2(\beta_1 b) - I_2(\beta_1 b) K_2(\beta_1 a) = 0$$

which has no real roots except the trivial solution, thus, the phase velocity of torsional waves is always greater than or equal to $(\frac{C_{44}}{\rho})^{1/2}$.

5.3 Motion independent of θ and z

When both the wave number k (i.e., for infinite wave length, $\lambda = 2\pi/k$) and n vanish, the frequency equation degenerates into three uncoupled families of modes, which may be identified as plane-strain extensional, plane-strain shear, and longitudinal shear.

The frequency equations for these three types of motion are, respectively, given by

$$\Delta_5 \Delta_6 \Delta_7 = 0. \tag{5.4}$$

The elements a_{ij} in (5.4) are given by (4.2) of fixed boundary conditions and (4.4) of mixed boundary conditions, with $k \rightarrow 0$ (i.e., for infinite wave length, $\lambda = 2\pi/k$), $n = 0$ and the appropriate simplifications outlined in (5.1). Furthermore, the Z and W are either J or Y functions, in accordance to Table 1 since $\rho\omega^2 > k^2 C_{33}$.

$$\Delta_5 = \begin{vmatrix} a_{13} & a_{15} \\ a_{53} & a_{55} \end{vmatrix} = 0, \quad \Delta_6 = \begin{vmatrix} a_{44} & a_{48} \\ a_{84} & a_{88} \end{vmatrix} = 0,$$

$$\Delta_7 = \begin{vmatrix} a_{34} & a_{38} \\ a_{74} & a_{78} \end{vmatrix} = 0.$$

The first of (5.4) for orthotropic thick cylinders, which includes transverse isotropy as a special case.

6 Frequency equation for solid circular cylinder

So far, we have considered the frequency equations for various types of motions of hollow circular cylinders. It is a trivial matter to deduce from this analysis the corresponding frequency equations for a solid circular cylinder. In the latter case, the inner radius $a \rightarrow 0$ and furthermore, the Bessel functions K and Y result in unbounded stresses and displacement at the origin $r = 0$. Hence all the coefficients a_{ij} involving a and the W functions must vanish and the frequency equation for the solid circular cylinder reduces to

$$\Delta_8 = \begin{vmatrix} a_{51} & a_{52} & a_{53} & a_{54} \\ a_{61} & a_{62} & a_{63} & a_{64} \\ a_{71} & a_{72} & a_{73} & a_{74} \\ a_{81} & a_{82} & a_{83} & a_{84} \end{vmatrix} = 0. \tag{6.1}$$

The elements a_{ij} in (6.1) are given by (4.2) of fixed boundary conditions and (4.4) of mixed boundary conditions, with $a = 0$. Furthermore, the Z and W are either J or Y functions, in accordance to Table 1. where, an interesting degenerate case of (6.1) is that of axially symmetric motions (i.e., $n = 0$). The frequency equation for this type of motion reduces to

$$\Delta_9 = \begin{vmatrix} a_{51} & a_{52} & a_{53} \\ a_{61} & a_{62} & a_{63} \\ a_{81} & a_{82} & a_{83} \end{vmatrix} \tag{6.2}$$

for mixed boundary conditions:

$$\left. \begin{aligned} a_{43} &= \left[2 \left(\frac{n}{\bar{b}} \right) \left\{ -\alpha_3 J_{n+1}(\alpha_3 \bar{b}) \right. \right. \\ &\quad \left. \left. + \frac{(n-1)}{\bar{b}} J_n(\alpha_3 \bar{b}) \right\} \right], \\ a_{45} &= \left[2 \left(\frac{n}{\bar{b}} \right) \left\{ -\alpha_1 Y_{n+1}(\alpha_1 \bar{b}) \right. \right. \\ &\quad \left. \left. + \frac{(n-1)}{\bar{b}} Y_n(\alpha_1 \bar{b}) \right\} \right], \\ a_{53} &= [\alpha_3^2 + d_3 \varepsilon Q' + R' e_3] J_n(\alpha_3 \bar{a}), \\ a_{55} &= [\alpha_1^2 + d_1 \varepsilon Q' + R' e_1] Y_n(\alpha_1 \bar{a}) \end{aligned} \right\} \tag{6.3}$$

for fixed boundary conditions:

$$\left. \begin{aligned} a_{43} &= J_n(\alpha_3 \bar{a}), \\ a_{45} &= Y_n(\alpha_1 \bar{a}), \\ a_{53} &= [\alpha_3^2 + d_3 \varepsilon Q' + R' e_3] J_n(\alpha_3 \bar{b}), \\ a_{55} &= [\alpha_1^2 + d_1 \varepsilon Q' + R' e_1] Y_n(\alpha_1 \bar{b}). \end{aligned} \right\} \quad (6.4)$$

If we assume now that the cross-sectional dimensions of the cylinder are small as compared to the length (i.e., $\gamma_1 b \ll 1$, $\gamma_2 b \ll 1$), an approximate value of the frequency of longitudinal waves in a bar can be obtained. Representing the Bessel functions in (6.3) as power series in $\gamma_i b$, a detailed analysis indicates that this type of motion can occur only when the frequency ϖ lies in the interval $k^2 C_{44} < \rho \varpi^2 < k^2 C_{33}$. When first terms only are retained in the power series expansions, the frequency ϖ is approximated by the expression

$$\rho \varpi^2 = k^2 C_{33} - \left[(k^2 C_{13}^2) / (C_{11} - C_{66}) \right]$$

where, ($C = \varpi/k$) is the velocity of the waves which propagated along the bar takes the form

$$C = \left[(C_{11} C_{33} - C_{66} C_{33}^2) / \rho (C_{11} - C_{66}) \right]^{1/2}.$$

For the special case of the isotropic cylinder $C_{11} = C_{33}$, $C_{12} = C_{13}$, $C_{66} = C_{44} = (C_{11} - C_{12})/2$ and the velocity C becomes

$$C = [C_{44} (2C_{11} - 4C_{44}) / \rho (C_{11} - C_{44})]^{1/2}.$$

In terms of the Lamé constants λ , μ , this expression reduces to

$$C = [\mu (3\lambda + 2\mu) / \rho (\lambda + \mu)]^{1/2} = (E/\rho)^{1/2}$$

where, $\lambda + 2\mu = C_{11}$, $\mu = C_{44}$ and E is Young’s modulus. This is the result in this investigations of longitudinal vibrations of bars. If more-accurate values of the frequency ϖ are desired, it would appear to be more efficient to go directly to the exact frequency (6.2) rather than perform the tedious analyses required in obtaining higher-order approximations in the manner outlined above.

7 Numerical results and discussion

The numerical results for the frequency equation are computed for the wet bone. Since the frequency equation is transcendental in nature, there are an infinite number of roots for the frequency equation. The results of frequency versus wave length are plotted in Figs. 1–7 for bones (transversely isotropic materials) for several values of n the number of circumferential waves. It is note that, since the determinantal (4.2) and (4.4) is transcendental in nature, there are an infinite number of modes for each value of $n = 1, 2, 3, \dots$. In most cases, the results of the approximate theory shown in Figs. 1–3, indicated the oscillation of the dispersion curve for the flexural mode ($n = 1, 2$) is quite low at smaller wave lengths and for larger wave lengths. It is notes that, three modes (under mixed boundary conditions, $n = 2$) the frequency fixed with the increasing of the wave lengths in the range $20 \leq \lambda \leq 50$, see Fig. 4. The roots are obtained for the flexural mode ($n = 1, 2$) in the cases of fixed boundary condition and mixed boundary condition are plotted and presented in Figs. 5, 6.

Consider the flexural mode $n = 2$, for various values of wave lengths, the frequencies, are obtained from frequency equation, the dispersion curves for dry bone [24] and wet bone are represented in Fig. 7. To study the effect of fluid part and the free charges of the fluid phase of the wet bone tissue, the dotted line represents the dispersion curve for the poroelastic case of dry bone, and the continuous line represents the dispersion curve for the poroelastic case of the wet bone. It is found that the two curves deviate quite high in the range $9 \leq \lambda \leq 20$. But they almost coincide in the range $20 \leq \lambda \leq 50$.

The dimensionless angular frequency Ω and parameter δ are defined in the following way

$$\Omega = \frac{\varpi}{2\pi} \frac{h}{\sqrt{(C_{66}/\rho)}}, \quad \delta = \frac{h}{\lambda}, \quad k = \frac{2\pi}{\lambda}$$

where, h and λ are, respectively, the thickness of the hollow cylinder and k is the wave length. The values of the elastic constants of the bone are taken from [17], see Table 1, it is summarized for the approximate geometry of the femur and the material constants in Gaussian units which are used in the computations. The poroelastic constant is evaluated from the expression given by Lang [18].

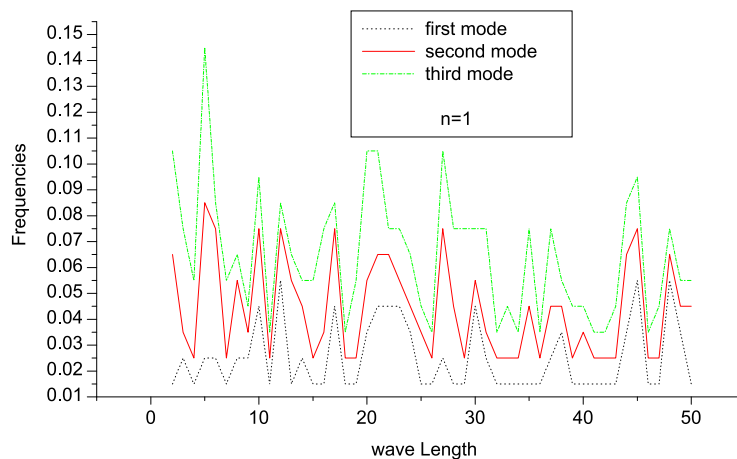


Fig. 1 Variations of the three modes frequencies respect wave length if $n = 1$

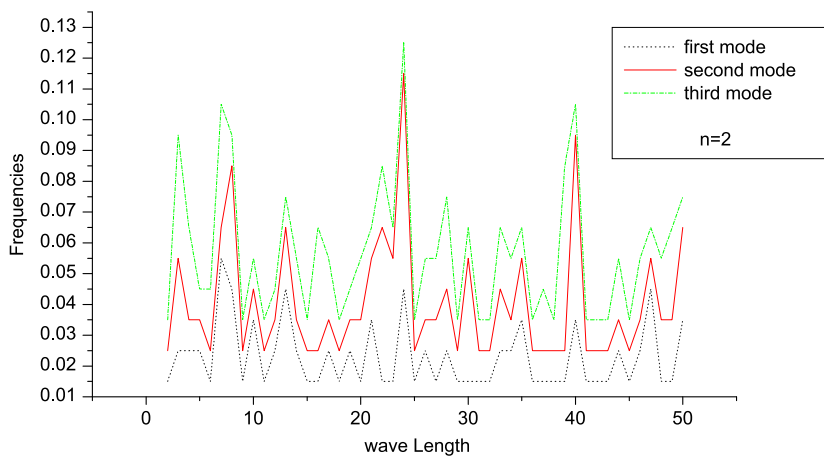


Fig. 2 Variations of the three modes frequencies respect wave length if $n = 2$

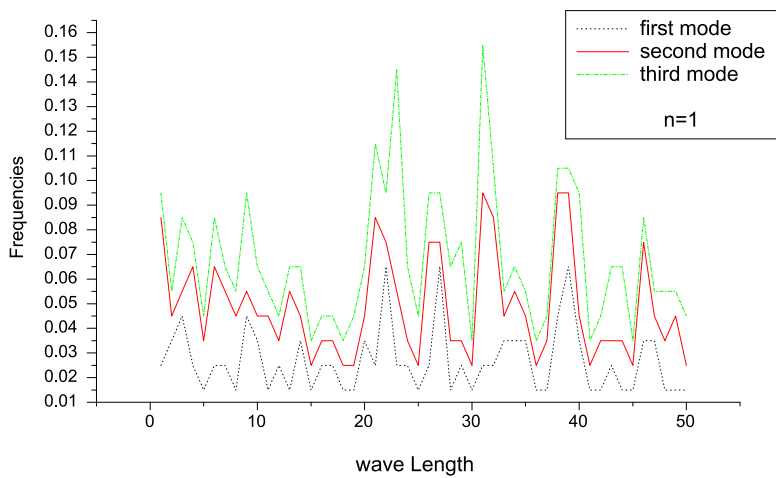


Fig. 3 Variations of the three modes frequencies respect wave length if $n = 1$

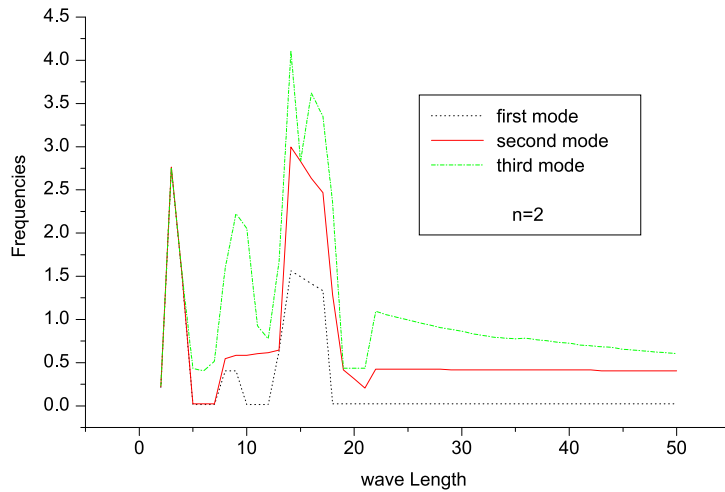


Fig. 4 Variations of the three modes frequencies respect wave length if $n = 2$

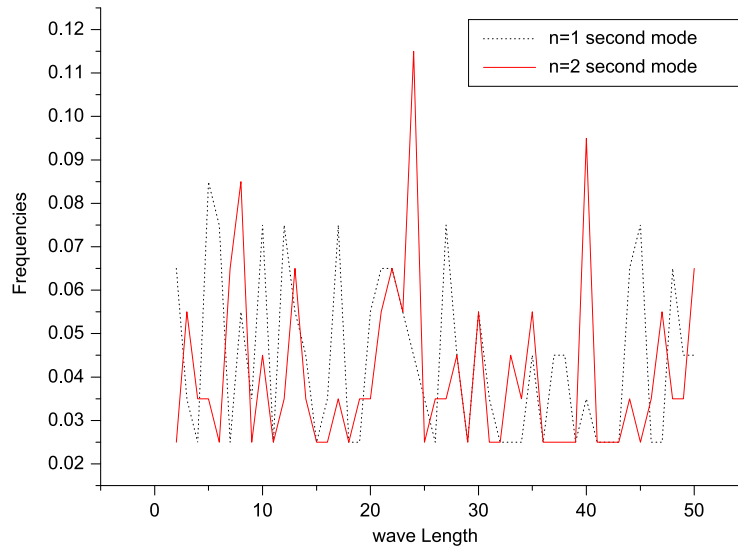


Fig. 5 Variations of the second mode frequencies respect wave length if $(n = 1, 2)$

Table 1 The approximate geometry of the femur and the material constants in Gaussian units

C_{11}	C_{12}	C_{13}	C_{33}	C_{44}	a	b	h
2.12	0.95	1.02	3.76	0.75	0.8	1.4	0.6

$$Q = f \left(1 - f - \frac{\delta}{\chi} \right) \left(\gamma + \delta + \frac{\delta^2}{\chi} \right),$$

$$R = \frac{f^2}{\left(\gamma + \delta + \frac{\delta^2}{\chi} \right)}$$

where, f is the porosity, and γ, δ, χ are related by Young’s modulus and the Poisson’s ratio. The expressions for χ, δ, γ are given by $\chi = 3(1 - 2\nu)/E$; $\delta = 0.6\chi$; and $\gamma = f(C_1 - \delta)$ where C_1 is taken to be zero for the incompressibility of the fluid. The porosity of the human bone in the age group 35–40 years is taken to be 0.24 [19]. In order to evaluate one more poroelastic constant it is assumed that $M/Q \cong C_{12}/C_{13}$ as the value M is not provided. Since the fluid in general is isotropic, it is taken that $b_{rr} = b_{zz}$. The density of the fluid in the poro-space,

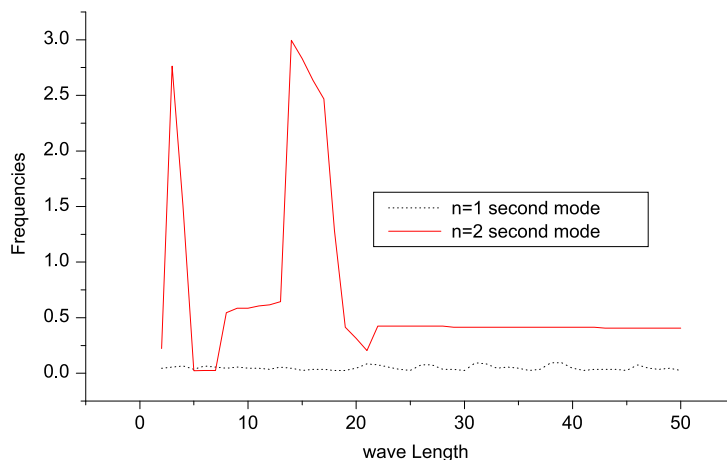


Fig. 6 Variations of the second mode frequencies respect wave length if ($n = 1, 2$)

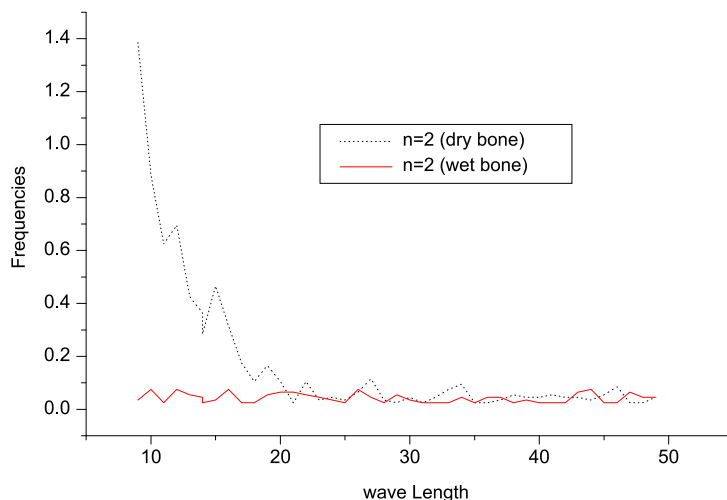


Fig. 7 Variations of the dry and wet bones frequencies respect wave length if $n = 2$

permeability of the medium and mass density of the bone are taken from [20].

In this work, we have studied the wave propagation in an infinite piezoelectric hollow cylinder of crystal class 6. We adopted the analysis of [21] and [22], and the solution of the problem was expressed in terms of a fluid part. The resulting dispersion relation has been solved numerically. Other researchers in the past have investigated this problem without succeeding to obtain an analytical solution. Gtizelsu and Saha [23] have obtained results for the wave propagation in the diaphysis of the dry femur (long bone) due to a mechanical stress wave. However, they have ignored the

effect of a fluid part on the stresses and presented numerical results only. Also, Fotiadis et al. [7] investigated wave propagation modeling in human long bones, they have ignored the effect of a fluid part on the stresses.

In addition to the other researchers we have investigated three modes and we have considered the four different cases (motion Independent of Z , motion independent on θ , motion independent on θ and Z , frequency equation for solid circular cylinder), resulting for those types of solutions of the characteristic (4.2) and (4.4) obtained for piezoelectric cylinder which are simplifications of the general problem.

8 Conclusions

In this paper, the wave propagation of a poroelastic bone with circular cylindrical cavity subjected to certain boundary condition is considered. The frequency equation is obtained by considering the material as transversely isotropic in nature. The numerical results are carried out and compared for the wet bone as a poroelastic material and dry bone. The conclusions of the paper are classified as follow:

- (1) For very large wave lengths, dispersion curves for flexural modes $n = 1, 2$ deviate and vibration are displayed graphically and very announced.
- (2) The frequency equation must be separated into three frequency ranges because of the changing nature of the Bessel functions involved.
- (3) As the wave length approaches infinity, the plane-strain vibrations become uncoupled from the longitudinal shear vibrations. These two types of motion become coupled for a non-infinity wave lengths.
- (4) For flexural motions ($n = 1, 2$), the coupled radial and axial motions are completely uncoupled from the pure torsional motions.
- (5) When both the wave length is infinity and if $n = 1, 2$, the three displacement potential functions f, g_1 and g_2 generate three uncoupled families of modes that may be identified as plane-strain extensional, plane-strain shear, and longitudinal shear, respectively.
- (6) The characteristic frequency (4.2) and (4.4) for the hollow cylinder can readily be reduced to that for the solid cylinder on taking the limit $a \rightarrow 0$.
- (7) The results can be specialized to the case of the isotropic cylinder by the following transformations:

$$C_{11} = C_{33}, \quad C_{12} = C_{13},$$

$$C_{66} = C_{44} = (C_{11} - C_{12})/2, \tag{8.1}$$

$$\gamma_2 \rightarrow \beta_1, \quad \lambda_1 \rightarrow -k, \quad \lambda_2 k \rightarrow q^2.$$
- (8) The results for approximate frequency of longitudinal vibrations of a long solid bar obtained for a generalized case of a transversely isotropic solid cylinder.
- (9) Finally, the results obtained compare well with the results obtained by Abd-Alla and Mahmoud [24] in the case of dry bone under analogous conditions

as it is shown in Fig. 7 for the case of a piezoelectric cylinder and the numerical results of the characteristic equation derived here are presented and illustrated graphically.

Appendix A

$$a_{11} = [\alpha_1^2 + d_1 \varepsilon Q' + R' e_1] J_n(\alpha_1 \bar{a}),$$

$$a_{12} = [\alpha_2^2 + d_2 \varepsilon Q' + R' e_2] J_n(\alpha_2 \bar{a}),$$

$$a_{13} = [\alpha_3^2 + d_3 \varepsilon Q' + R' e_3] J_n(\alpha_3 \bar{a}),$$

$$a_{14} = 0,$$

$$a_{15} = [\alpha_1^2 + d_1 \varepsilon Q' + R' e_1] Y_n(\alpha_1 \bar{a}),$$

$$a_{16} = [\alpha_2^2 + d_2 \varepsilon Q' + R' e_2] Y_n(\alpha_2 \bar{a}),$$

$$a_{17} = [\alpha_3^2 + d_3 \varepsilon Q' + R' e_3] Y_n(\alpha_3 \bar{a}),$$

$$a_{18} = 0,$$

$$a_{21} = \alpha_1 \left[\left(\frac{n}{\bar{a}\alpha_1} \right) J_n(\alpha_1 \bar{a}) - J_{n+1}(\alpha_1 \bar{a}) \right],$$

$$a_{22} = \alpha_2 \left[\left(\frac{n}{\bar{a}\alpha_2} \right) J_n(\alpha_2 \bar{a}) - J_{n+1}(\alpha_2 \bar{a}) \right],$$

$$a_{23} = \alpha_3 \left[\left(\frac{n}{\bar{a}\alpha_3} \right) J_n(\alpha_3 \bar{a}) - J_{n+1}(\alpha_3 \bar{a}) \right],$$

$$a_{24} = \left(\frac{n}{\bar{a}} \right) J_n(\alpha_4 \bar{a}),$$

$$a_{25} = \alpha_1 \left[\left(\frac{n}{\bar{a}\alpha_1} \right) Y_n(\alpha_1 \bar{a}) - Y_{n+1}(\alpha_1 \bar{a}) \right],$$

$$a_{26} = \alpha_2 \left[\left(\frac{n}{\bar{a}\alpha_2} \right) Y_n(\alpha_2 \bar{a}) - Y_{n+1}(\alpha_2 \bar{a}) \right],$$

$$a_{27} = \alpha_3 \left[\left(\frac{n}{\bar{a}\alpha_3} \right) Y_n(\alpha_3 \bar{a}) - Y_{n+1}(\alpha_3 \bar{a}) \right],$$

$$a_{28} = \left(\frac{n}{\bar{a}} \right) Y_n(\alpha_8 \bar{a}),$$

$$a_{31} = \left(\frac{n}{\bar{a}} \right) J_n(\alpha_1 \bar{a}), \quad a_{32} = \left(\frac{n}{\bar{a}} \right) J_n(\alpha_2 \bar{a}),$$

$$a_{33} = \left(\frac{n}{\bar{a}} \right) J_n(\alpha_3 \bar{a}),$$

$$a_{34} = \alpha_4 \left[\left(\frac{n}{\bar{a}\alpha_4} \right) J_n(\alpha_4 \bar{a}) - J_{n+1}(\alpha_4 \bar{a}) \right],$$

$$\begin{aligned}
 a_{35} &= \left(\frac{n}{\bar{a}}\right) Y_n(\alpha_1 \bar{a}), & a_{36} &= \left(\frac{n}{\bar{a}}\right) Y_n(\alpha_2 \bar{a}), \\
 a_{37} &= \left(\frac{n}{\bar{a}}\right) Y_n(\alpha_3 \bar{a}), \\
 a_{38} &= \alpha_4 \left[\left(\frac{n}{\bar{a}\alpha_4}\right) Y_n(\alpha_4 \bar{a}) - Y_{n+1}(\alpha_4 \bar{a}) \right], \\
 a_{41} &= J_n(\alpha_1 \bar{a}), & a_{42} &= J_n(\alpha_2 \bar{a}), \\
 a_{43} &= J_n(\alpha_3 \bar{a}), & a_{44} &= 0, \\
 a_{45} &= Y_n(\alpha_1 \bar{a}), & a_{46} &= Y_n(\alpha_2 \bar{a}), \\
 a_{47} &= Y_n(\alpha_3 \bar{a}), & a_{48} &= 0, \\
 a_{51} &= \left[\alpha_1^2 + d_1 \varepsilon Q' + R' e_1 \right] J_n(\alpha_1 \bar{b}), \\
 a_{52} &= \left[\alpha_2^2 + d_2 \varepsilon Q' + R' e_2 \right] J_n(\alpha_2 \bar{b}), \\
 a_{53} &= \left[\alpha_3^2 + d_3 \varepsilon Q' + R' e_3 \right] J_n(\alpha_3 \bar{b}), & a_{54} &= 0, \\
 a_{55} &= \left[\alpha_1^2 + d_1 \varepsilon Q' + R' e_1 \right] Y_n(\alpha_1 \bar{b}), \\
 a_{56} &= \left[\alpha_2^2 + d_2 \varepsilon Q' + R' e_2 \right] Y_n(\alpha_2 \bar{b}), \\
 a_{57} &= \left[\alpha_3^2 + d_3 \varepsilon Q' + R' e_3 \right] Y_n(\alpha_3 \bar{b}), & a_{58} &= 0, \\
 a_{61} &= \alpha_1 \left[\left(\frac{n}{\bar{b}\alpha_1}\right) J_n(\alpha_1 \bar{b}) - J_{n+1}(\alpha_1 \bar{b}) \right], \\
 a_{62} &= \alpha_2 \left[\left(\frac{n}{\bar{b}\alpha_2}\right) J_n(\alpha_2 \bar{b}) - J_{n+1}(\alpha_2 \bar{b}) \right], \\
 a_{63} &= \alpha_3 \left[\left(\frac{n}{\bar{b}\alpha_3}\right) J_n(\alpha_3 \bar{b}) - J_{n+1}(\alpha_3 \bar{b}) \right], \\
 a_{64} &= \left(\frac{n}{\bar{b}}\right) J_n(\alpha_4 \bar{b}), \\
 a_{65} &= \alpha_1 \left[\left(\frac{n}{\bar{b}\alpha_1}\right) Y_n(\alpha_1 \bar{b}) - Y_{n+1}(\alpha_1 \bar{b}) \right], \\
 a_{66} &= \alpha_2 \left[\left(\frac{n}{\bar{b}\alpha_2}\right) Y_n(\alpha_2 \bar{b}) - Y_{n+1}(\alpha_2 \bar{b}) \right], \\
 a_{67} &= \alpha_3 \left[\left(\frac{n}{\bar{b}\alpha_3}\right) Y_n(\alpha_3 \bar{b}) - Y_{n+1}(\alpha_3 \bar{b}) \right], \\
 a_{68} &= \left(\frac{n}{\bar{b}}\right) Y_n(\alpha_8 \bar{b}), \\
 a_{71} &= \left(\frac{n}{\bar{b}}\right) J_n(\alpha_1 \bar{b}), & a_{72} &= \left(\frac{n}{\bar{b}}\right) J_n(\alpha_2 \bar{b}), \\
 a_{73} &= \left(\frac{n}{\bar{b}}\right) J_n(\alpha_3 \bar{b}),
 \end{aligned}$$

$$\begin{aligned}
 a_{74} &= \alpha_4 \left[\left(\frac{n}{\bar{b}\alpha_4}\right) J_n(\alpha_4 \bar{b}) - J_{n+1}(\alpha_4 \bar{b}) \right], \\
 a_{75} &= \left(\frac{n}{\bar{b}}\right) Y_n(\alpha_1 \bar{b}), & a_{76} &= \left(\frac{n}{\bar{b}}\right) Y_n(\alpha_2 \bar{b}), \\
 a_{77} &= \left(\frac{n}{\bar{b}}\right) Y_n(\alpha_3 \bar{b}), \\
 a_{78} &= \alpha_4 \left[\left(\frac{n}{\bar{b}\alpha_4}\right) Y_n(\alpha_4 \bar{b}) - Y_{n+1}(\alpha_4 \bar{b}) \right], \\
 a_{81} &= J_n(\alpha_1 \bar{b}), & a_{82} &= J_n(\alpha_2 \bar{b}), \\
 a_{83} &= J_n(\alpha_3 \bar{b}), & a_{84} &= 0, \\
 a_{85} &= Y_n(\alpha_1 \bar{b}), & a_{86} &= Y_n(\alpha_2 \bar{b}), \\
 a_{87} &= Y_n(\alpha_3 \bar{b}), & a_{88} &= 0
 \end{aligned}$$

where, ($j = 1, 2, 3$).

Appendix B

$$\begin{aligned}
 a_{11} &= \left[\alpha_1^2 + d_1 \varepsilon Q' + R' e_1 \right] J_n(\alpha_1 \bar{b}), \\
 a_{12} &= \left[\alpha_2^2 + d_2 \varepsilon Q' + R' e_2 \right] J_n(\alpha_2 \bar{b}), \\
 a_{13} &= \left[\alpha_3^2 + d_3 \varepsilon Q' + R' e_3 \right] J_n(\alpha_3 \bar{b}), & a_{14} &= 0, \\
 a_{15} &= \left[\alpha_j^2 + d_1 \varepsilon Q' + R' e_1 \right] Y_n(\alpha_1 \bar{b}), \\
 a_{16} &= \left[\alpha_2^2 + d_2 \varepsilon Q' + R' e_2 \right] Y_n(\alpha_2 \bar{b}), \\
 a_{17} &= \left[\alpha_3^2 + d_3 \varepsilon Q' + R' e_3 \right] Y_n(\alpha_3 \bar{b}), & a_{18} &= 0, \\
 a_{21} &= \left[2 \left(\frac{n}{\bar{b}}\right)^2 \bar{C}_{66} - \alpha_1^2 \bar{C}_{11} - \bar{C}_{13} d_1 \varepsilon \right. \\
 &\quad \left. - \bar{M} e_1 - \left(\frac{2}{\bar{b}}\right)^2 n \bar{C}_{66} \right] \\
 &\quad \times J_n(\alpha_1 \bar{b}) - \left(\frac{2}{\bar{b}}\right)^2 n \bar{C}_{66} \alpha_1 J_{n+1}(\alpha_1 \bar{b}), \\
 a_{22} &= \left[2 \left(\frac{n}{\bar{b}}\right)^2 \bar{C}_{66} - \alpha_2^2 \bar{C}_{11} - \bar{C}_{13} d_2 \varepsilon \right. \\
 &\quad \left. - \bar{M} e_2 - \left(\frac{2}{\bar{b}}\right)^2 n \bar{C}_{66} \right] \\
 &\quad \times J_n(\alpha_2 \bar{b}) - \left(\frac{2}{\bar{b}}\right)^2 n \bar{C}_{66} \alpha_2 J_{n+1}(\alpha_2 \bar{b}),
 \end{aligned}$$

$$a_{23} = \left[2 \left(\frac{n}{\bar{b}} \right)^2 \bar{C}_{66} - \alpha_3^2 \bar{C}_{11} - \bar{C}_{13} d_3 \varepsilon \right. \\ \left. - \bar{M} e_3 - \left(\frac{2}{\bar{b}} \right)^2 n \bar{C}_{66} \right] \\ \times J_n(\alpha_3 \bar{b}) - \left(\frac{2}{\bar{b}} \right)^2 n \bar{C}_{66} \alpha_3 J_{n+1}(\alpha_3 \bar{b}),$$

$$a_{24} = 2 \left(\frac{n}{\bar{b}} \right) \bar{C}_{66} [-\alpha_4 J_{n+1}(\alpha_4 \bar{b}) \\ + \frac{(n-1)}{\bar{b}} J_n(\alpha_4 \bar{b})],$$

$$a_{25} = \left[2 \left(\frac{n}{\bar{b}} \right)^2 \bar{C}_{66} - \alpha_1^2 \bar{C}_{11} - \bar{C}_{13} d_1 \varepsilon \right. \\ \left. - \bar{M} e_1 - \left(\frac{2}{\bar{b}} \right)^2 n \bar{C}_{66} \right] \\ \times Y_n(\alpha_1 \bar{b}) - \left(\frac{2}{\bar{b}} \right)^2 n \bar{C}_{66} \alpha_1 Y_{n+1}(\alpha_1 \bar{b}),$$

$$a_{26} = \left[2 \left(\frac{n}{\bar{b}} \right)^2 \bar{C}_{66} - \alpha_2^2 \bar{C}_{11} - \bar{C}_{13} d_2 \varepsilon \right. \\ \left. - \bar{M} e_2 - \left(\frac{2}{\bar{b}} \right)^2 n \bar{C}_{66} \right] \\ \times Y_n(\alpha_2 \bar{b}) - \left(\frac{2}{\bar{b}} \right)^2 n \bar{C}_{66} \alpha_2 Y_{n+1}(\alpha_2 \bar{b}),$$

$$a_{27} = \left[2 \left(\frac{n}{\bar{b}} \right)^2 \bar{C}_{66} - \alpha_3^2 \bar{C}_{11} - \bar{C}_{13} d_3 \varepsilon \right. \\ \left. - \bar{M} e_3 - \left(\frac{2}{\bar{b}} \right)^2 n \bar{C}_{66} \right] \\ \times Y_n(\alpha_3 \bar{b}) - \left(\frac{2}{\bar{b}} \right)^2 n \bar{C}_{66} \alpha_3 Y_{n+1}(\alpha_3 \bar{b}),$$

$$a_{28} = 2 \left(\frac{n}{\bar{b}} \right) \bar{C}_{66} [-\alpha_4 Y_{n+1}(\alpha_4 \bar{b}) \\ + \frac{(n-1)}{\bar{b}} Y_n(\alpha_4 \bar{b})],$$

$$a_{31} = [\alpha_1 (d_1 + \varepsilon)] \left[\left(\frac{n}{\bar{b} \alpha_1} \right) J_n(\alpha_1 \bar{b}) - J_{n+1}(\alpha_1 \bar{b}) \right],$$

$$a_{32} = [\alpha_2 (d_2 + \varepsilon)] \left[\left(\frac{n}{\bar{b} \alpha_2} \right) J_n(\alpha_2 \bar{b}) - J_{n+1}(\alpha_2 \bar{b}) \right],$$

$$a_{33} = [\alpha_3 (d_3 + \varepsilon)] \left[\left(\frac{n}{\bar{b} \alpha_3} \right) J_n(\alpha_3 \bar{b}) - J_{n+1}(\alpha_3 \bar{b}) \right],$$

$$a_{34} = \left(\frac{n}{\bar{b}} \right) J_n(\alpha_4 \bar{b}),$$

$$a_{35} = [\alpha_1 (d_1 + \varepsilon)] \left[\left(\frac{n}{\bar{b} \alpha_1} \right) Y_n(\alpha_1 \bar{b}) - Y_{n+1}(\alpha_1 \bar{b}) \right],$$

$$a_{36} = [\alpha_2 (d_2 + \varepsilon)] \left[\left(\frac{n}{\bar{b} \alpha_2} \right) Y_n(\alpha_2 \bar{b}) - Y_{n+1}(\alpha_2 \bar{b}) \right],$$

$$a_{37} = [\alpha_3 (d_3 + \varepsilon)] \left[\left(\frac{n}{\bar{b} \alpha_3} \right) Y_n(\alpha_3 \bar{b}) - Y_{n+1}(\alpha_3 \bar{b}) \right],$$

$$a_{38} = \left(\frac{n}{\bar{b}} \right) Y_n(\alpha_4 \bar{b}),$$

$$a_{41} = \left[2 \left(\frac{n}{\bar{b}} \right) \left\{ -\alpha_1 J_{n+1}(\alpha_1 \bar{b}) \right. \right. \\ \left. \left. + \frac{(n-1)}{\bar{b}} J_n(\alpha_1 \bar{b}) \right\} \right],$$

$$a_{42} = \left[2 \left(\frac{n}{\bar{b}} \right) \left\{ -\alpha_2 J_{n+1}(\alpha_2 \bar{b}) \right. \right. \\ \left. \left. + \frac{(n-1)}{\bar{b}} J_n(\alpha_2 \bar{b}) \right\} \right],$$

$$a_{43} = \left[2 \left(\frac{n}{\bar{b}} \right) \left\{ -\alpha_3 J_{n+1}(\alpha_3 \bar{b}) \right. \right. \\ \left. \left. + \frac{(n-1)}{\bar{b}} J_n(\alpha_3 \bar{b}) \right\} \right],$$

$$a_{44} = \left(\frac{1}{\bar{b}} \right)^2 \left[2 \bar{b} \alpha_4 J_{n+1}(\alpha_4 \bar{b}) \right. \\ \left. + (\alpha_4^2 \bar{b}^2 + 2n^2 - 2n) J_n(\alpha_4 \bar{b}) \right],$$

$$a_{45} = \left[2 \left(\frac{n}{\bar{b}} \right) \left\{ -\alpha_1 Y_{n+1}(\alpha_1 \bar{b}) \right. \right. \\ \left. \left. + \frac{(n-1)}{\bar{b}} Y_n(\alpha_1 \bar{b}) \right\} \right],$$

$$a_{46} = \left[2 \left(\frac{n}{\bar{b}} \right) \left\{ -\alpha_2 Y_{n+1}(\alpha_2 \bar{b}) \right. \right. \\ \left. \left. + \frac{(n-1)}{\bar{b}} Y_n(\alpha_2 \bar{b}) \right\} \right],$$

$$a_{47} = \left[2 \left(\frac{n}{\bar{b}} \right) \left\{ -\alpha_3 Y_{n+1}(\alpha_3 \bar{b}) \right. \right. \\ \left. \left. + \frac{(n-1)}{\bar{b}} Y_n(\alpha_3 \bar{b}) \right\} \right],$$

$$\begin{aligned}
 a_{48} &= \left(\frac{1}{\bar{b}}\right)^2 \left[2\bar{b}\alpha_4 Y_{n+1}(\alpha_4 \bar{b}) + (\alpha_4^2 \bar{b}^2 + 2n^2 - 2n) Y_n(\alpha_4 \bar{b}) \right], \\
 a_{51} &= [\alpha_1^2 + d_1 \varepsilon Q' + R' e_1] J_n(\alpha_1 \bar{a}), \\
 a_{52} &= [\alpha_2^2 + d_2 \varepsilon Q' + R' e_2] J_n(\alpha_2 \bar{a}), \\
 a_{53} &= [\alpha_3^2 + d_3 \varepsilon Q' + R' e_3] J_n(\alpha_3 \bar{a}), \quad a_{54} = 0, \\
 a_{55} &= [\alpha_1^2 + d_1 \varepsilon Q' + R' e_1] Y_n(\alpha_1 \bar{a}), \\
 a_{56} &= [\alpha_2^2 + d_2 \varepsilon Q' + R' e_2] Y_n(\alpha_2 \bar{a}), \\
 a_{57} &= [\alpha_3^2 + d_3 \varepsilon Q' + R' e_3] Y_n(\alpha_3 \bar{a}), \quad a_{58} = 0, \\
 a_{61} &= \alpha_1 \left[\left(\frac{n}{\bar{a}\alpha_1}\right) J_n(\alpha_1 \bar{a}) - J_{n+1}(\alpha_1 \bar{a}) \right], \\
 a_{62} &= \alpha_2 \left[\left(\frac{n}{\bar{a}\alpha_2}\right) J_n(\alpha_2 \bar{a}) - J_{n+1}(\alpha_2 \bar{a}) \right], \\
 a_{63} &= \alpha_3 \left[\left(\frac{n}{\bar{a}\alpha_3}\right) J_n(\alpha_3 \bar{a}) - J_{n+1}(\alpha_3 \bar{a}) \right], \\
 a_{64} &= \left(\frac{n}{\bar{a}}\right) J_n(\alpha_4 \bar{a}), \\
 a_{65} &= \alpha_1 \left[\left(\frac{n}{\bar{a}\alpha_1}\right) Y_n(\alpha_1 \bar{a}) - Y_{n+1}(\alpha_1 \bar{a}) \right], \\
 a_{66} &= \alpha_2 \left[\left(\frac{n}{\bar{a}\alpha_2}\right) Y_n(\alpha_2 \bar{a}) - Y_{n+1}(\alpha_2 \bar{a}) \right], \\
 a_{67} &= \alpha_3 \left[\left(\frac{n}{\bar{a}\alpha_3}\right) Y_n(\alpha_3 \bar{a}) - Y_{n+1}(\alpha_3 \bar{a}) \right], \\
 a_{68} &= \left(\frac{n}{\bar{a}}\right) Y_n(\alpha_4 \bar{a}), \\
 a_{71} &= \left(\frac{n}{\bar{a}}\right) J_n(\alpha_1 \bar{a}), \quad a_{72} = \left(\frac{n}{\bar{a}}\right) J_n(\alpha_2 \bar{a}), \\
 a_{73} &= \left(\frac{n}{\bar{a}}\right) J_n(\alpha_3 \bar{a}), \\
 a_{74} &= \alpha_4 \left[\left(\frac{n}{\bar{a}\alpha_4}\right) J_n(\alpha_4 \bar{a}) - J_{n+1}(\alpha_4 \bar{a}) \right], \\
 a_{75} &= \left(\frac{n}{\bar{a}}\right) Y_n(\alpha_1 \bar{a}), \quad a_{76} = \left(\frac{n}{\bar{a}}\right) Y_n(\alpha_2 \bar{a}), \\
 a_{77} &= \left(\frac{n}{\bar{a}}\right) Y_n(\alpha_3 \bar{a}), \\
 a_{78} &= \alpha_4 \left[\left(\frac{n}{\bar{a}\alpha_4}\right) Y_n(\alpha_4 \bar{a}) - Y_{n+1}(\alpha_4 \bar{a}) \right],
 \end{aligned}$$

$$\begin{aligned}
 a_{81} &= J_n(\alpha_1 \bar{a}), & a_{82} &= J_n(\alpha_2 \bar{a}), \\
 a_{83} &= J_n(\alpha_3 \bar{a}), & a_{84} &= 0, \\
 a_{85} &= Y_n(\alpha_1 \bar{a}), & a_{86} &= Y_n(\alpha_2 \bar{a}), \\
 a_{87} &= Y_n(\alpha_3 \bar{a}), & a_{88} &= 0
 \end{aligned}$$

where, $(j = 1, 2, 3)$.

References

1. Natali AN, Meroi EA (1989) A review of the biomechanical properties of bone as a material. *J Biomed Eng* 11(4):266–276
2. Thompson GA, Young DR, Orne D (1976) In vivo determination of mechanical properties of human ulna by means of mechanical impedance tests: experimental results and improved mathematical model. *Med Biol Eng* 14:253–262
3. Doherty WP, Boville EG, Wilson EL (1974) Evaluation of the use of resonant frequencies to characterize physical properties of long bones. *J Biomech* 7:559–561
4. Jurist JM (1970) In vivo determination of the elastic response of bone-I. Method of ulnar resonant frequency determination. *Phys Med Biol* 15:417–426
5. Papathanasopoulou VA, Fotiadis DI, Foutsitzi G, Massalas CV (2002) A poroelastic bone model for internal remodeling. *Int J Eng Sci* 40:511–530
6. Fotiadis DI, Foutsitzi G, Massalas CV (2000) Wave propagation in human long bones of arbitrary cross-section. *Int J Eng Sci* 38(14):1553–1591
7. Fotiadis DI, Foutsitzi G, Massalas CV (1999) Wave propagation modeling in human long bones. *Acta Mech* 137:65–81
8. Sebaa N, Fellah Z, Lauriks W, Depollier C (2006) Application of fractional calculus to ultrasonic wave propagation in human cancellous bone. *Signal Process* 86(10):2668–2677
9. Padilla F, Bossy E, Haiat G, Jenson F, Laugier P (2006) Numerical simulation of wave propagation in cancellous bone, ultrasonic propagation in cancellous bone. *Ultrasonics* 44:e239–e243
10. Haeat G, Padilla F, Barkmann R, Gluer CC, Laugier P (2006) Numerical simulation of the dependence of quantitative ultrasonic parameters on trabecular bone micro architecture and elastic constants. *Ultrasonics* 44:e289–e294
11. Pithious M, Lasaygues P, Chabrand P (2002) An alternative ultrasonic method for measuring the elastic properties of cortical bone. *J Biomech* 35:961–968
12. Kaczmarek M, Kubik J, Pakula M (2002) Short ultrasonic waves in cancellous bone. *Ultrasonics* 40:95–100
13. Levitsky SP, Bergman RM, Haddad J (2004) Wave propagation in a cylindrical viscous layer between two elastic shells. *Int J Eng Sci* 42:2079–2086
14. Tadeu A, Mendes PA, António J (2006) 3D elastic wave propagation modelling in the presence of 2D fluid-filled thin inclusions. *Eng Anal Bound Elem* 30:176–193
15. Paul HS, Murali VM (1992) Wave propagation in cylindrical poroelastic bone with cavity. *Int J Eng Sci* 30:1629–1635

16. Qina Q, Qua C, Ye J (2005) thermoelectroelastic solutions for surface bone remodeling under axial and transverse loads. *Biomaterials* 26:6798–6810
17. Biot MA (1962) Mechanics of deformation and acoustic propagation in porous media. *J Appl Phys* 33(4):1482–1498
18. Lang SB (1970) Ultrasonic method for measuring elastic coefficients of bone and results on fresh and dried bovine bones. *IEEE Trans Biomed Eng* 17:101–105
19. Davis CF (1970) On the mechanical properties of bone and a poroelastic theory of stresses in bone. PhD Thesis, Univ of Delaware
20. Ghista DN (1979) *Applied Physiological Mechanics*. Ellis Horwood, Chichester, pp 31–96
21. Salzstein RA, Pollack SR, Mak AFT, Petrov N (1987) Electromechanical potentials in cortical bone a continuum approach. *J Biomech* 20:261–270
22. Ding H, Chenbuo L (1996) General solutions for coupled equations for piezoelectric media. *Int J Solids Struct* 16:2283–2298
23. Güzelsu N, Saha S (1981) Electro-mechanical wave propagation in long bones. *J Biomech* 14:9–33
24. Mahmoud SR (2010) Wave propagation in cylindrical poroelastic dry bones. *Appl Math Inf Sci* 4(2):209–226
25. Protopappas VC, Vavva MG, Fotiadis DI, Malizos KN (2008) Ultrasonic monitoring of bone fracture healing. *IEEE Trans Ultrason Ferroelectr Freq Control* 55(6):1243–1255
26. Vavva MG, Protopappas VC, Fotiadis DI, Malizos KN (2008) Ultrasound velocity measurements on healing bones using the external fixation pins: a two-dimensional simulation study. *J Serb Soc Comput Mech* 2(2):1–15
27. Kauffman JJ (2008) Ultrasonic guided waves in bone. *IEEE Trans Ultrason Ferroelectr Freq Control* 55(6):1205–1218
28. Moilanen P (2008) Ultrasonic guided waves in bone. *IEEE Trans Ultrason Ferroelectr Freq Control* 55(6):1277–1286
29. Vavva MG, Protopappas VC, Gergidis LN, Charalambopoulos A, Fotiadis DI, Polyzos D (2009) Velocity dispersion of guided waves propagating in a free gradient elastic plate: Application to cortical bone. *J Acoust Soc Am* 125(5):3414–3427